Int. J. Electrochem. Sci., 7 **(2012)** 7295 - 7303

International Journal of
ELECTROCHEMICAL
SCIENCE
www.electrochemsci.org

Detonation-synthesized Nanodiamond as a Stable Support of Pt Electrocatalyst for Methanol Electrooxidation

L.Y. Bian[1,2], *Y.H. Wang*[1], *J.B. Zang*[1,*], *F.W. Meng*[1], *Y.L. Zhao*[1]

[1] State Key Laboratory of Metastable Material Science and Technology, College of Material Science and Engineering, Yanshan University, Qinhuangdao 066004, China
[2] College of Physics and Chemistry, Henan Polytechnic University, Jiaozuo, Henan 454000, China
[*]E-mail: diamondzjb@163.com

Received: 29 June 2012 / *Accepted:* 19 July 2012 / *Published:* 1 August 2012

Detonation-synthesized nanodiamond (DND) supported platinum electrocatalyst (Pt/DND) were fabricated using a microwave-heating polyol method. The Pt/DND nanocomposites were characterized by energy-dispersive spectroscopy, transmission electron microscopy, and X-ray diffraction. The Pt nanoparticles with the mean size of 3-4 nm were highly dispersed on DND supports. The electrochemical measurements demonstrated that the Pt/DND nanocomposite prepared exhibited high electrocatalytic activity for methanol electrooxidation reaction just like other sp^2-bonded carbon supported catalyst.

Keywords: Undoped nanodiamond; Microwave; Platinum; Electrocatalyst; Methanol.

1. INTRODUCTION

Detonation-synthesized nanodiamond (DND) is a novel carbon material. It not only has the properties of diamond, for example the outstanding hardness and antiwear, high thermal conductivity etc. [1], but also possesses the features of a nano-scale material, such as an ultrafine particle size and a giant specific surface area as well as large numbers of surface defects [2]. Recently, other than traditional polishing and grinding, there has been great interest in the use of DND particles and powders in biological applications, for example for intracellular imaging [3] and drug delivery [4].

Most recently DND powders have been incorporated into electrode, and exhibited the electrochemical activity in aqueous and nonaqueous solutions. Our group reported the electrochemical properties of 5 nm DND in aqueous solution containing the ferricyanide–ferrocyanide redox couple [5] or the nitrite [6]. Holt et al attributed the electrochemical response of undoped DND to the oxidation and reduction of surface states [7]. The electrochemical properties combining with the giant specific

surface area and the excellent stabilization render DND to be interested in electrocatalysis field as a support material [8].

Nanoscaled Pt and Pt-based alloy are well known to be good electrocatalysts in the fuel cell applications [9-16]. The catalytic activity is strongly dependent on the particle shape, size and the particle size distribution [17, 18]. Conventional preparation techniques based on wet impregnation and chemical reduction of metal precursors can not provide satisfied control of particle shape and size [18]. Consequently, a great deal of efforts was done to develop alternative synthesis methods based on microemulsions [19], sonochemistry [20, 21] and microwave irradiation [22-25], all of which are in principle more conducive to produce colloids and clusters on the nanoscale, and with greater uniformity.

Microwave heating through dielectric losses is fast and simple, uniform, energy efficient, and has been used in preparative chemistry and materials synthesis [26, 27]. Previous studies [28-30] demonstrated that Pt/XC-72 carbon, Pt/CNTs and Pt/graphite nanofibers prepared by microwave polyol process showed very good electrocatalytic properties for methanol electrooxidation reaction (MOR).

In the present work, Pt nanoparticles were deposited on DND powders using microwave-heating method. The electrocatalytic effects of the prepared Pt/DND toward MOR were investigated.

2. EXPERIMENTAL SECTION

2.1 Reagents

The 5 nm DND powder are supplied by Element Six Ltd. The platinum precursor (H_2PtCl_6•$6H_2O$), ethylene glycol (EG), and sulfuric acid (H_2SO_4) were purchased from Shanghai Chemical Products Ltd. Deionized water was used to prepare the solutions and high-purity nitrogen gas was also used in the experiments.

2.2 Preparation of Pt/DND nanocompsite

The preparation of Pt/DND was carried out in EG solutions of H_2PtCl_6 precursor salts by microwave-heating. First, 2.0 mL of 0.055 mol/L aqueous H_2PtCl_6 solution were mixed with 25 mL of EG in a 100 mL beaker. Then the mixture was ultrasonically mixed with 5, 10, 15, 20, or 40 mg of DND powder respectively. The beaker was placed in a microwave oven and heated for 200 s at 800 W. and then the suspensions were washed by acetone and distilled water, dried at room temperature. The samples of Pt/DND-1, Pt/DND-2, Pt/DND-3, Pt/DND-4, and Pt/DND-5 respectively corresponding to the addition of DND quality as 5, 10, 15, 20, and 40 mg in the mixtures were obtained.

2.3 Characterizations of Pt/DND nanocompsite

X-ray diffraction (XRD) was used to determine the crystalline structure of the samples. JEM2010 High Resolution Transmission Electron Microscopy (HRTEM) was used to characterize the morphology of the catalysts.

2.4 Electrochemical measurement

Electrocatalytic activities of Pt/DND electrocatalysts for MOR and electrochemical properties of DND were measured by cyclic voltammetry (CV) and chronoamperometry (CA) using a CHI660A electrochemical workstation. A conventional three-electrode system was used, consisting of a Pt/DND (or DND) electrode as a working electrode, a platinum coil auxiliary electrode, and an Ag/AgCl electrode as the reference electrode. The experiments were conducted at 25 °C. The working electrode was obtained in the following way: The Pt/DND catalysts or DND (10 mg) were dispersed in 10 mL ethanol by ultrasonication for 30 min to achieve a 1.0 mg/mL suspension, and one drop of the suspension was directly cast on the surface of glassy carbon electrode (7.07 mm^2) and evaporated at room temperature. 10 μL Nafion solution (5 wt.%, Du Pont) was sprayed on the catalyst surface dried at room temperature to form a protective layer and avoid a loss of catalyst during the test. The active specific surface area of the Pt particles was calculated according to a hydrogen adsorption/desorption curve. All electrolyte solutions were deaerated by high purity nitrogen for 30 min prior to any electrochemical measurement.

3. RESULTS AND DISCUSSION

3.1 Electrochemical stability of DND

For the electrochemical oxidation of the supports, the CVs of DND were recorded in 0.5 mol/L H_2SO_4 before and after 500 cycling between 0 and 1.2 V, as shown in Figure 1. For typical sp^2 carbon materials, an increased area of electrochemical characteristic curves means a deteriorated stability of supports due to remarkable changes of surface or chemical states. So the increased area difference before and after cycling is often used as a criterion of stability of supports [31, 32]. In Figure 1, there was little variation in area of CVs after 500 cycles, indicating that DND had a high resistant to electrochemical oxidation.

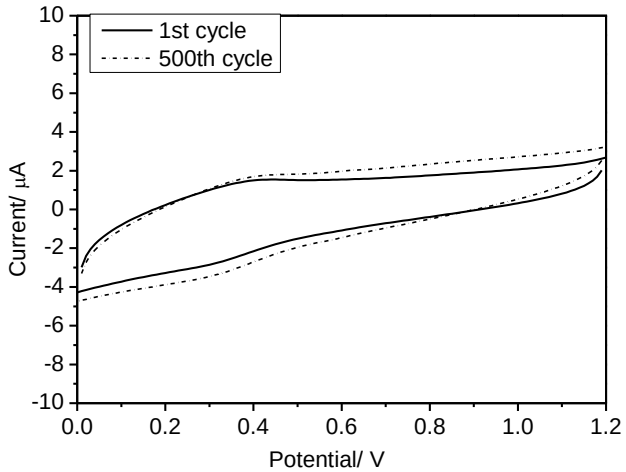

Figure 1. CVs of DND electrode in 0.5 mol/L H_2SO_4 before and after 500 cycles between 0 and 1.2 V, at a scan rate of 50 mV/s.

3.2 XRD characterizations of Pt/DND nanocomposite

The structure of the Pt/DND composite was characterized by XRD, as shown in Figure 2. XRD patterns confirmed the presence of crystalline Pt nanoparticles with characteristic peaks at 2θ values of 39.8°, 46.2°, 67.4°, and 81.2°, corresponding to the reflection planes (1 1 1), (2 0 0), (2 2 0), and (3 1 1), respectively. It could be indexed to face-centered cubic platinum, and the widening of the peaks implied the nanoscale of the Pt particles. The weaker peaks appeared at 43.98°, 75.28°, and 91.68°, corresponding to the (1 1 1), (2 2 0), and (3 1 1) cubic diamond planes. The low intensity was attributed to the cover of Pt nanoparticles on the surface.

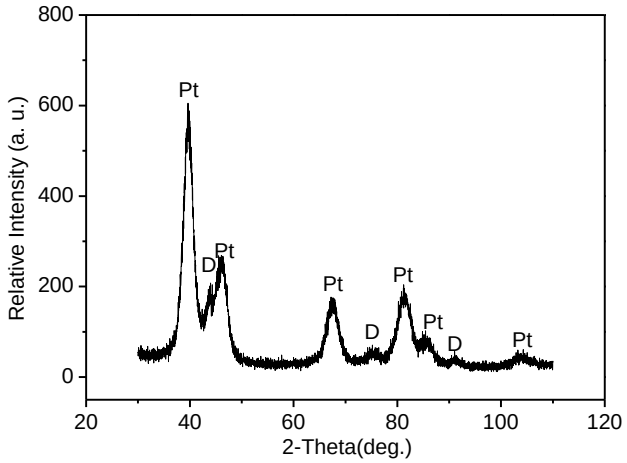

Figure 2. XRD patterns of Pt/DND nanocomposite

3.3 Transmission Electron Microscopy characterizations of Pt/DND nanocomposite

Figure 3 shows the Transmission Electron Microscopy (TEM) and the HRTEM images of the Pt/DND nanocomposite prepared using the microwave polyol process. In Figure 3a and 3b, it can be seen that the DNDs have the size of 4–10 nm, and show a strong tendency of agglomeration. Pt particles with the size of 3–4 nm are uniformly dispersed on the rough surfaces of agglomerated DND. DND and Pt particles can be distinguished easily according to image contrasts because of the different atomic numbers.

Figure 3c and 3d show the HRTEM images of Pt/DND nanocomposites, in which the morphology of Pt particles can be seen clearly. Face-centered cubic metal Pt is of a cubooctahedral structure consisting of (1 1 1) and (1 0 0) facets bounded by edge atom rows that are like the topmost rows of the (1 1 0) surface [33]. The lattice parameters of 0.22 and 0.196 nm correspond to (1 1 1) and (2 0 0) facets of Pt, respectively. In addition, the lattice parameter of 0.206 nm, which is identified to be equal to that of DND are also found in Figure 3d. The form and size of the particles can not be well defined due to the agglomeration effect of the DND particles.

The composite structure is schematically shown in Figure 4. DND particles were core aggregates of the particles of approximately 100–200 nm, rather than isolated 5 nm particles. After

microwave heated, Pt nanoparticles are uniformly dispersed on the rough surfaces of agglomerated DND powders. DND powers on agglomerated state still had giant specific surface area, which can be provided for deposition of catalyst. We measured the BET surface area, which was 226 m^2/g.

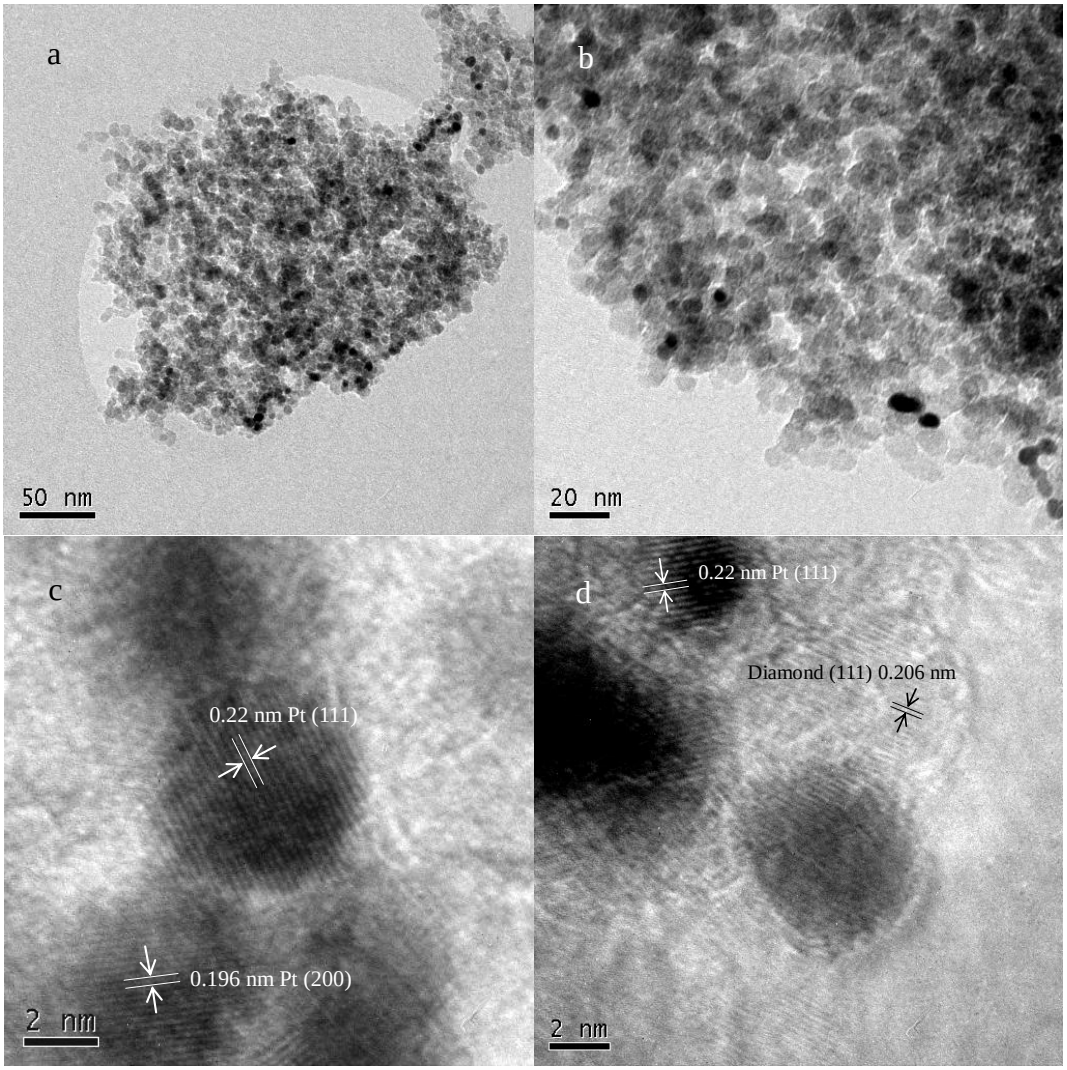

Figure 3. TEM (a,b) and HRTEM (c,d) images of Pt/DND nanocomposites

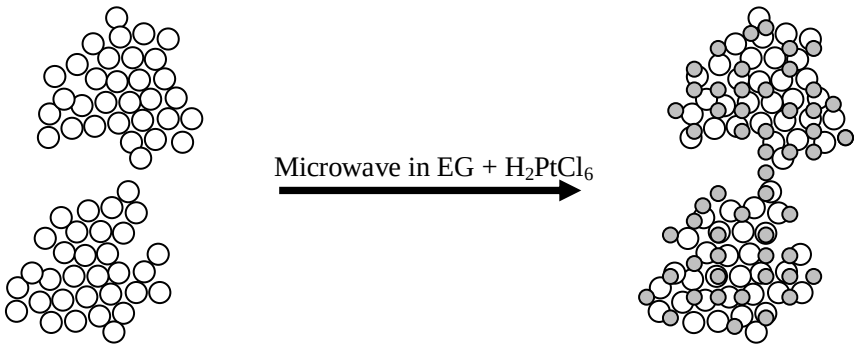

Figure 4. Schematic illustration showing structure of Pt/DND nanocomposite

3.4 Active specific surface area of Pt/DND nanocomposite

Figure 5 presents the CV curve of Pt/DND-1 catalysts in a 0.5 mol/L H_2SO_4 solution at a scan rate of 50 mV/s. Three pairs of reversible peaks corresponding to the hydrogen adsorption and desorption are observed in the potential range between -0.3 V and 0 V (vs Ag/AgCl), rather than a single broad peak, which is indicative of multiple exposed crystallographic planes. Hydrogen adsorption/desorption is a powerful technique to determine the active surface area of a Pt electrode [34]. The integrated intensity of the peaks represents the number of Pt sites available for hydrogen adsorption/desorption, that is, the actual surface area. By means of CV curve in Figure 5, the electrochemical surface areas (A_{EL}) in m^2/g of platinum were calculated from the following formula assuming a correspondence value of 0.21 mC/cm^2, a value generally admitted for polycrystalline Pt electrodes [35] and the Pt loading. The formual is A_{EL} (m^2/g Pt) = Q_H / (0.21×10^{-3} C×g Pt), where A_{EL} is the active specific surface area of Pt particles obtained electrochemically, Q_H the amount of charge exchanged during the electroadsorption of hydrogen atoms on Pt and DND is the Coulomb, and the Pt loading of Pt/DND-1 is 1.896 μg/cm^2. The obtained A_{EL} of the Pt/DND-1 catalysts was 57.14 m^2/g Pt, corresponding approximately to that of Pt/C catalysts or Pt/CNTs with Pt nanoparticles of the same size [17, 36]. This result indicated that Pt was electrochemically available on the DND nanoparticle surface like on the surface of the sp^2-bonded carbon materials.

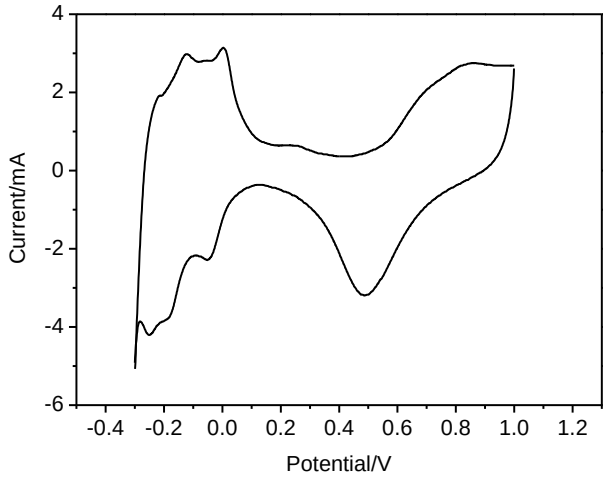

Figure 5. A hydrogen electroadsorption CV curve for Pt/DND nanocomposite in 0.5 mol/L H_2SO_4 at a scan rate of 50 mV/s

3.5 MOR over Pt/DND nanocomposite

The electrocatalytic activity of methanol oxidation on DND and Pt/DND-1 catalysts was characterized by CV curves (Figure 6) in 1.0 mol/L CH_3OH + 0.5 mol/L H_2SO_4 at 50 mV/s.

From Figure 6, the typical background current of the DND electrode (inset in Figure 6) can be determined, and no current peaks of MOR can be observed. It indicated that the DND substrate had no obvious electrocatalytic activity for MOR. However, two peaks of MOR are seen at 0.64 and 0.43 V

on the Pt/DND-1 electrode. The CV features proved that the catalytic activity of the Pt/DND nanocomposite towards MOR and were in agreement with those reported literatures [37, 38]. The forward oxidation peak current (I_f) of the MOR is 1.232×10^{-2} A, while the reverse anodic peak (I_b) during the back scan of the MOR in CV curves is 1.253×10^{-2} A. Goodenough et al. [39] attributed this I_b to the removal of the incompletely oxidized CO-like species formed in the forward scan, defining the ratio of I_f to I_b, I_f/I_b, to describe the catalyst tolerance to carbonaceous species accumulation. A high I_f/I_b ratio indicates good oxidation of methanol to CO_2 during the anodic scan and a small quantity of accumulation of CO-like residues on the catalyst surface. It is found that the I_f/I_b of Pt/DND catalysts (1.01) is higher than that of Pt/C (0.76) reported in the literature [40]. The enhancement in I_f/I_b for the Pt/DND catalysts might be ascribed to the oxygen functional surface states of DND, which could improve the oxidation of CO-like residues.

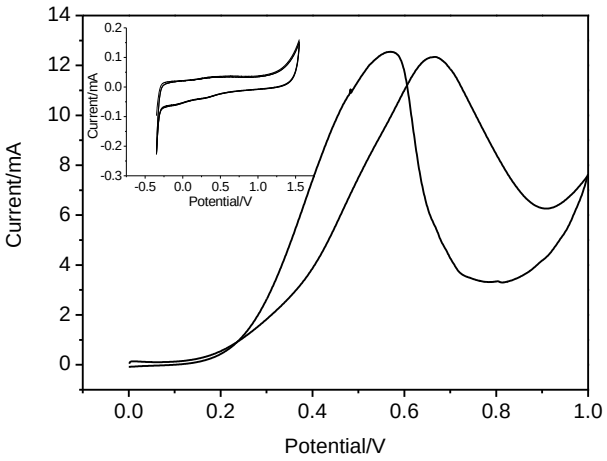

Figure 6. CV curves on the DND (inset) and Pt/DND-1 catalysts in 1.0 mol/L CH_3OH + 0.5 mol/L H_2SO_4 at a scan rate of 50 mV/s.

3.6 Influence of Pt-Loading Content on the MOR

Figure 7 shows typical CV (a) and (CA) (b) curves for the MOR in 1.0 mol/L CH_3OH + 0.5 mol/L H_2SO_4 recorded on Pt/DND-1, Pt/DND-2, Pt/DND-3, Pt/DND-4, and Pt/DND-5 catalysts electrodes respectively. It is observed that while the I_f of the MOR decreased with the reduction of Pt loading, the I_f/I_b changed slightly. The calculated electro-catalytic performance parameters of Pt/DND catalysts with different Pt loading are list in Table 1. On the Pt/DND-5 catalyst electrode, no current peaks of MOR were observed because of the extremely low Pt loading (0.237 $\mu g/cm^2$).

CA data were recorded at 0.6 V for 600 s as a measure of the catalyst deactivation. It can be seen that the MOR current of Pt/DND catalysts decays with time and reaches an apparent steady state at about 300 s. Moreover, the steady state current of the Pt/DND was found to increase with increased Pt loading.

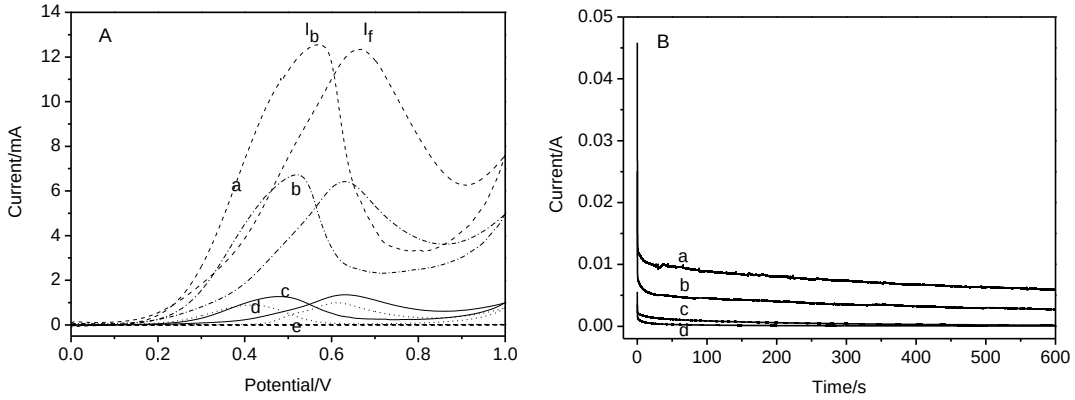

Figure 7. CV (A) and four CA (B) curves for the MOR in 1.0 mol/L CH_3OH + 0.5 mol/L H_2SO_4 recorded on Pt/DND-1 (a), Pt/DND-2 (b), Pt/DND-3 (c), Pt/DND-4 (d), and Pt/DND-5 (e) catalysts electrodes with a reducing Pt loading.

Table 1. Electrocatalytic Performance Parameters of As-Prepared Pt/DND toward MOR

sample	Pt loading ($\mu g/cm^2$)	peak current/mass (A/mg_{Pt})	I_f/I_b	I_f (mA)
Pt/DND-1	1.896	0.12	1.01	12.32
Pt/DND-2	0.948	0.08	0.95	6.41
Pt/DND-3	0.632	0.03	1.01	1.37
Pt/DND-4	0.474	0.03	1.11	1.01
Pt/DND-5	0.237	—	—	—

4. CONCLUSIONS

Pt/DND nanocomposites were fabricated using a microwave-heating polyol method, and the Pt particles were uniformly dispersed on the rough surface of DND aggregation. The size of the Pt particles was about 3–4 nm. The active specific surface area A_{EL} of Pt/DND with 1.896 $\mu g/cm^2$ Pt loading was 57.14 m^2/gPt, which corresponded approximately with Pt/C catalysts or Pt/CNTs with Pt nanoparticles of the same size. The Pt/DND composites exhibited good catalytic activity for MOR, and the I_f/I_b of Pt/DND catalysts (1.01) was higher than that of Pt/C (0.76).

ACKNOWLEDGMENT
This work was funded by the National Natural Science Foundation of China (Grant Nos. 50872119 and 50972125) and the Natural Science Foundation of Hebei Province (Grant Nos. E2010001187, E2011203126 and E2012203112). The authors also gratefully acknowledge financial and material support from Element Six Co..

References

1. B. V. Spitsyn, S. A. Denisov, N. A. Skorik, A. G. Chopurova, S. A. Parkaeva, L. D. Belyakova, and O. G. Larionov, *Diamond Relat. Mater.* 19 (2010)123.

2. N. Gibson, O. Shenderova, T. J. M. Luo, S. Moseenkov, V. Bondar, A. Puzyr, K. Purtov, Z. Fitzgerald, and D. W. Brenner, *Diamond Relat. Mater.* 18 (2009)620.
3. C.-C. Fu, H.-Y. Lee, K. Chen, T.-S. Lim, H.-Y. Wu, P.-K. Lin, P.-K. Wei, P.-H. Tsao, H.-C. Chang, and W. Fann, *Proc. Natl. Acad. Sci. U. S. A.* 104 (2007)727.
4. R. Lam, M. Chen, E. Pierstorff, H. Huang, E. Osawa, and D. Ho, *ACS Nano* 2 (2008)2095.
5. J. B. Zang, Y. H. Wang, S. Z. Zhao, L. Y. Bian, and J. Lu, *Diamond Relat. Mater.* 16 (2007)16.
6. L. H. Chen, J. B. Zang, Y. H. Wang, and L. Y. Bian, *Electrochim. Acta* 53 (2008)3442.
7. K. B. Holt, D. J. Caruana, and E. J. Millán-Barrios, *J. Am. Chem. Soc.* 131 (2009)11272.
8. L. Y. Bian, Y. H. Wang, J. B. Zang, J. K. Yu, and H. Huang, *J. Electroanal. Chem.* 644 (2010)85.
9. P. J. S. Prieto, A. P. Ferreira, P. S. Haddad, D. Zanchet, and J. M. C. Bueno, *J. Catal.* 276 (2010)351.
10. Y.-Y. Chu, Z.-B. Wang, D.-M. Gu, and G.-P. Yin, *J. Power Sources* 195 (2010)1799.
11. Z. Liu, X. Y. Ling, X. Su, J. Y. Lee, and L. M. Gan, *J. Power Sources* 149 (2005)1.
12. B. Abida, L. Chirchi, S. Baranton, T. W. Napporn, H. Kochkar, J.-M. Léger, and A. Ghorbel, *Appl. Catal. B: Environ.* 106 (2011)609.
13. J. R. C. Salgado, E. Antolini, and E. R. Gonzalez, *Appl. Catal. B: Environ.* 57 (2005)283.
14. K. Shimizu, J. S. Wang, I. F. Cheng, and C. M. Wai, *Energy & Fuels* 23 (2009)1662.
15. F. Su, C. K. Poh, Z. Tian, G. Xu, G. Koh, Z. Wang, Z. Liu, and J. Lin, *Energy & Fuels* 24 (2010)3727.
16. L. Yang, Y. Xiao, G. Zeng, S. Luo, S. Kuang, and Q. Cai, *Energy & Fuels* 23 (2009)3134.
17. X. Li, W. X. Chen, J. Zhao, W. Xing, and Z. D. Xu, *Carbon* 43 (2005)2168.
18. T. S. Armadi, Z. L. Wang, T. C. Green, A. Henglein, and M. A. El-Sayed, *Science* 272 (1996)1924.
19. Z. Liu, J. Y. Lee, M. Han, W. Chen, and L. M. Gan, *J. Mater. Chem.* 12 (2002)2453.
20. K. Okitsu, A. Yue, S. Tanabe, and H. Matsumoto, *Chem. Mater.* 12 (2000)3006.
21. T. Fujimoto, S. Teraushi, H. Umehara, I. Kojima, and W. Henderson, *Chem. Mater.* 13 (2001)1057.
22. W. Y. Yu, W. X. Tu, and H. F. Liu, *Langmuir* 15 (1999)6.
23. W. Y. Yu and H. Y. Liu, *Chem. Mater.* 12 (2000)564.
24. W. X. Tu and H. F. Liu, *J. Mater. Chem.* 10 (2000)2207.
25. S. Komarneni, D. S. Li, B. Newalkar, H. Katsuki, and A. S. Bhalla, *Langmuir* 18 (2002)5959.
26. A. Miyazaki, I. Balint, K. Aika, and Y. Nakano, *J. Catal.* 204 (2001)364.
27. S. A. Galema, *Chem. Soc, Rev.* 26 (1997)233.
28. W. X. Chen, J. Y. Lee, and Z. L. Liu, *Chem. Commun.* 0 (2002)2588.
29. J. Zhao, W. X. Chen, G. Han, Y. F. Zheng, and Z. D. Xu, *Chin. Chem. Lett.* 16 (2005)269.
30. W. X. Chen, J. Zhao, J. Y. Lee, and Z. L. Liu, *Mater. Chem. Phys.* 91 (2005)124.
31. J. Qi, S. Yan, Q. Jiang, Y. Liu, and G. Sun, *Carbon* 48 (2010)163.
32. J.-M. Lee, S.-B. Han, J.-Y. Kim, Y.-W. Lee, A.-R. Ko, B. Roh, I. Hwang, and K.-W. Park, *Carbon* 48 (2010)2290.
33. M. Arenz, K. J. J. Mayrhofer, V. Stamenkovic, B. B. Bilzanac, T. Tomoyuki, P. N. Ross, and N. M. Markovic, *J. Am. Chem. Soc.* 127 (2005)6819.
34. D. Kardash and C. Korzeniewski, *Langmuir* 16 (2000)8419.
35. J. Wang and G. M. Swain, *J. Electrochem. Soc.* 150 (2003)E24.
36. J. Zhao, P. Wang, W. Chen, R. Liu, X. Li, and Q. Nie, *J. Power Sources* 160 (2006)563.
37. P. K. Shen and Z. Tian, *Electrochim. Acta* 49 (2004)3107.
38. Z. Fu, W. Li, W. Zhang, F. Sun, Z. Zhou, and X. Xiang, *Int. J. Hydrogen Energy* 35 (2010)8101.
39. R. Mancharan and J. B. Goodenough, *J. Mater. Chem.* 2 (1992)875.
40. X. Ge, R. Wang, P. Liu, and Y. Ding, *Chem. Mater.* 19 (2007)5827